Extracellular potentials of axonal projections including terminations and bifurcations

Thomas McColgan, Hermann Wagner, Richard Kempter

June 29, 2015

Introduction

Extracellular field potentials (EFPs) in the brain were long thought to be primarily synaptic in origin (Buzsáki, Anastassiou, and Koch 2012). However, a number of recent data analysis and modeling studies have revealed that active, non-synaptic membrane currents can play a role in generating EFPs (Reimann et al. 2013).

It has been shown (Kuokkanen et al. 2010), that with sufficient spatial and temporal organization purely axonal extracellular fields can reach strengths on the order of several mV. Here we extend this finding to include more general axon bundles, including those recieving input with less temporal precision.

The aim of this study is to understand how the EFP is influenced by the anatomical structure of the axons which are the source of the potential. In particular, we explain how typical projection patterns in which an axon bundle widens and then terminates in its projection area affect the EFP.

Such axon bundles exist throughout the peripheral and central nervous system. (Examples...) The white matter of the brain can be viewed as an aglomeration of such bundles. (ref)

Based on a forward model of the extracellular field potential (Holt and Koch 1999,Gold et al. (2006)), we characterize three principal effects of axon bundle structure on the EFP, and demonstrate them using two models of varying complexity, as well as a set of electrophysiological recordings from the barn owl brain stem. These effects are elaborations of the properties of such bundles described in past (A. Gydikov et al. 1986,A. A. Gydikov and Trayanova (1986),Plonsey (1977)).

The study of the fields is relevant in many measurement methods which rely on the extracellular field potential. The relevance may also including noninvasive methods, where the underlying mechansms of far field generation are often poorly understood.

Relationship to CSD

- cite: rall, Rinzel, einevoll, Destexe, Brette, nunez&srinivasan, telenzuk, rattay&danner, cec email ref

Results

- Axonal projections generate a dipole-like field potential (**Fig 1A**)
  - long range
  - low frequency
  - Examples of phenomenology from literature
- General results for axonal projections :
  - The low-frequency (eg population rate pulse) parts are governed by the local density of bifurcations and terminations(**Fig 1B**)
  - The high-frequency (eg individual spikes, 'noise', neurophonic) parts are governed by the local fiber density(**Fig 1C**)
  - The low-frequency component exceeds the high-frequency component in reach (**Fig 2**)
- The barn owl neurophonic as an example that shows these properties(**Fig 3**)
  - The high-frequency component shows a steady increase in latency along the projections' depth, while the low-frequency can have stationary parts caused by sharp increases or decreases of fiber number (bifurcations or terminations).
  - These aspects are reflected in the model
- Ways of understanding the effect
  - Single AP along single axon(**Fig 4**)
  - Analytical model(**Fig 5**)

Discussion

- Relevance of Findings
  - Interpretation of CSD
    - Classical CSD: constant fiber density, variable currents
    - Here: variable fiber density, constant currents
  - Dipole has far field, ABR response?
- Compare to other auditory systems (Chicken NL, MSO)
  - Speculate on functional relevance of polarity shift (a la Rinzel & Goldwyn)
- compare to other fiber bundle systems

Methods

- Experimental Methods
- Multicompartment Model
- Analytical Model

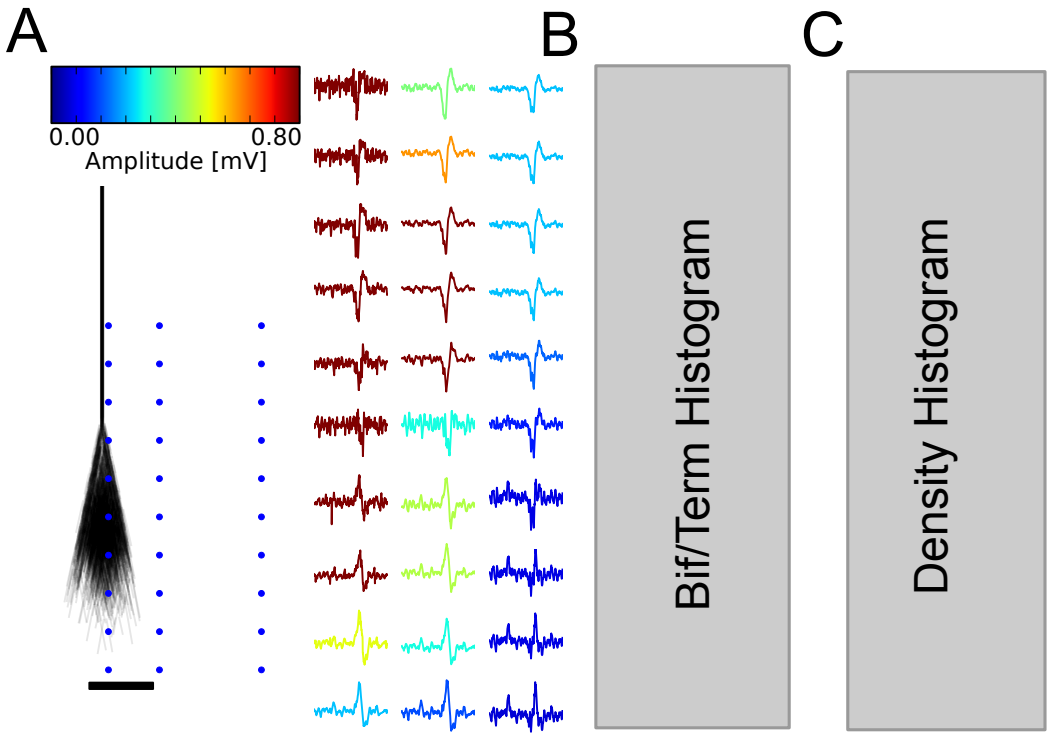

Figure 1: Axonal projections generate a dipole-like extracellular field potential. Extracellular evoked potential due to a pulse of activity in a generic fiber bundle. (**A**) shows the structure of the bundle, as well as EFP responses at various locations, indicated by blue dots. Scaling of traces indicated by colorbar. Relative strength of high-frequency noise relative to the low-frequency pulse decays with distance. The low frequency pulse switches polarity along the nerve bundles termination zone. (**B**) shows the density of bifurcations and terminations at varying depths, overlayed with the peak amplitude of the low frequency component. (**C**) shows the fiber density overlayed with the strength of the high-frequency EFP component.

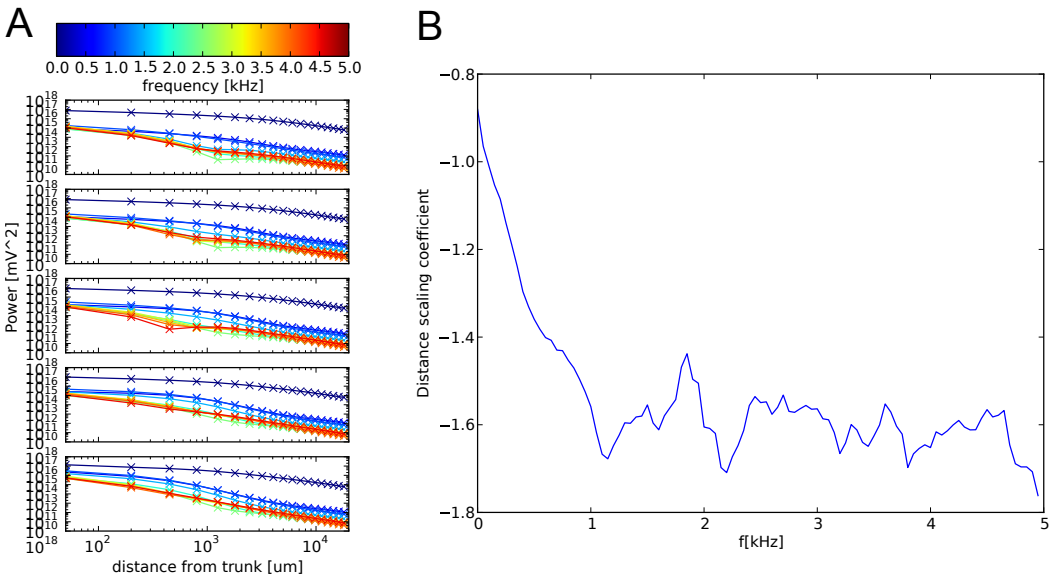

Figure 2: Low-frequency component of the axon bundle EFP exceeds high frequency in reach. (**A**) shows the behaviour of different spectral components (frequency indicated by colorbar) in a double logarithmic plot. The slope indicates the scaling coefficient in this frequency band. (**B**) shows this scaling coefficient for different frequencies. Low frequencies have the least negative coefficient, indicating the furthest reach.

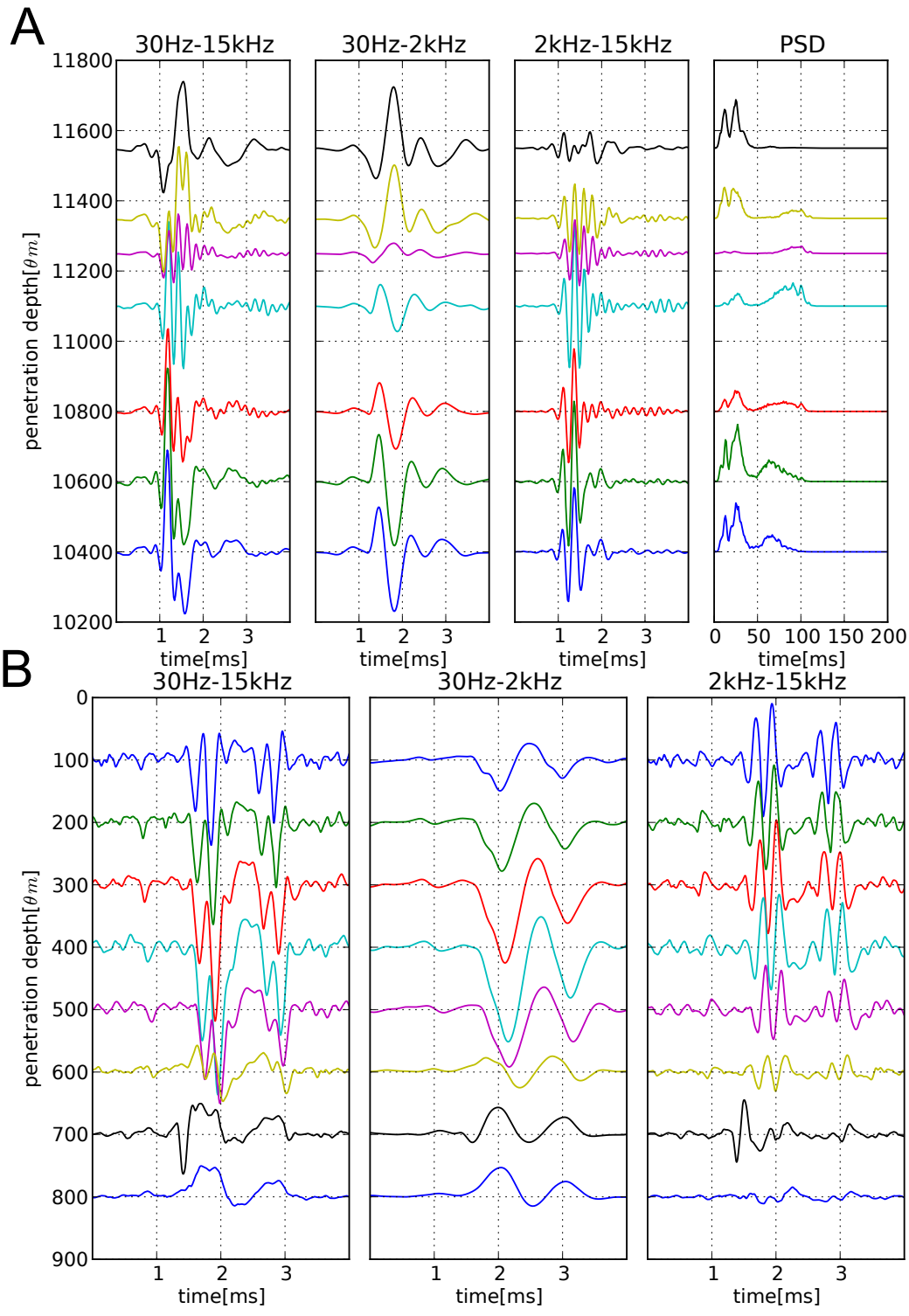

Figure 3: Data from the barn owl shows the expected behaviour predicted by the model. (**A**) shows data from the barn owls nucleus laminaris in response to an auditory click stimulus, compared to a simulation of the axonal structure and activation in (**B**). The click stimulus induces a pulse of activity in the afferent axon bundle. The low-frequency components (**Ab** and **Bb**) show the polarity reversal. The high frequency component (**Ac** and **Bc**, does not show such a reversal, but rather shows a steady increase in phase with depth.

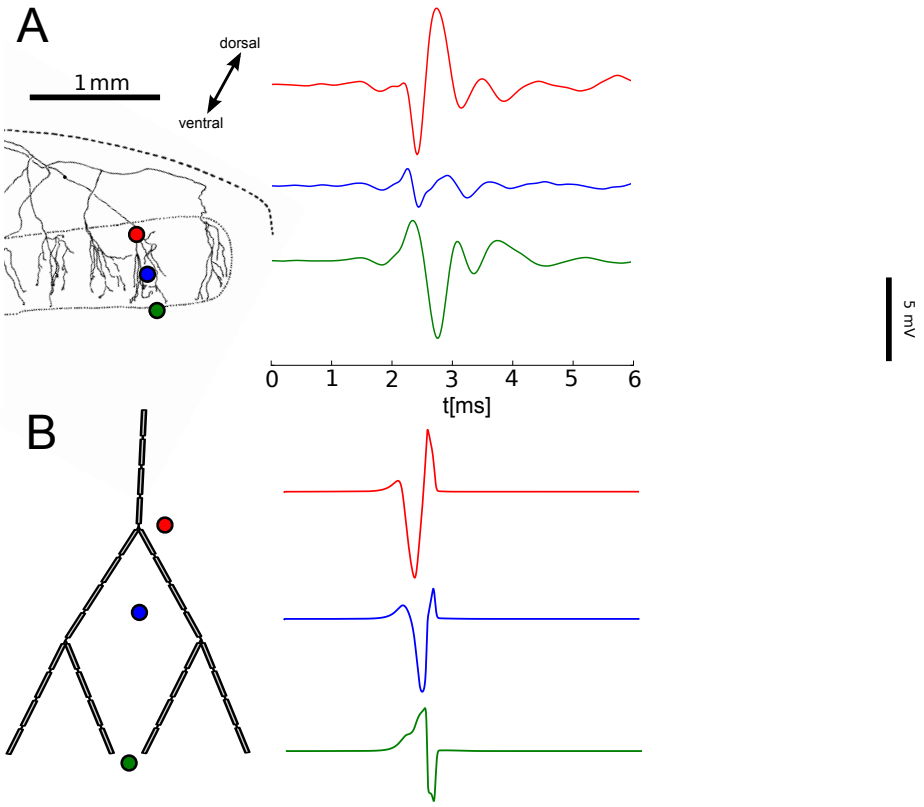

Figure 4: The dipolar behaviour can be understood by examining individual action potentials on a single axon tree. Comparing the low frequency owl data (**A**) to a single axon and action potential in model (**B**) shows a similar behaviour. In particular, the potential at a termination and that at a bifurcation (red and green curves in **B**) are approximately inverted.

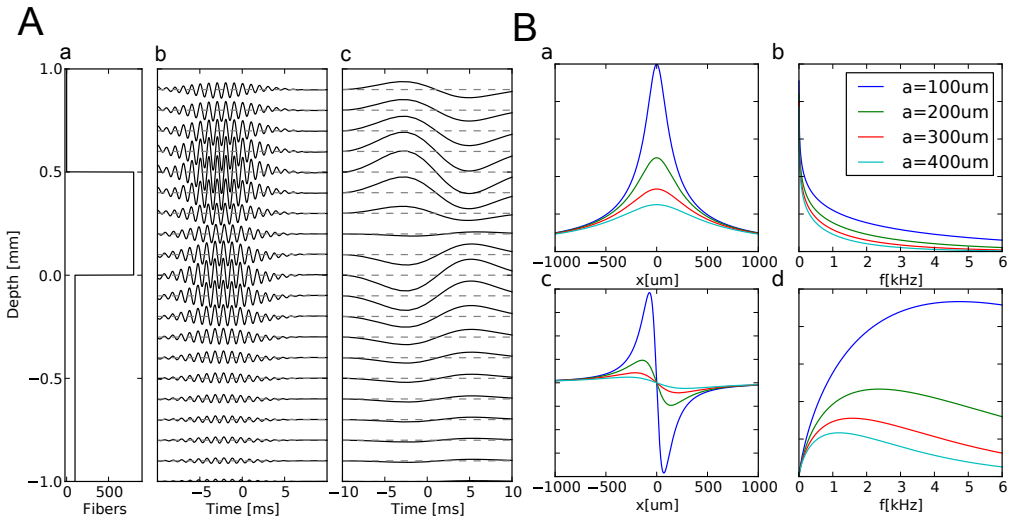

Figure 5: Analytical model of the axon bundle potential explains the effects observed in the numerical model and example data. (**A**) shows the behaviour of a simplified fiber bundle with a piecewise constant fiber density (**Aa**). The high frequency component (**Ab**) shows no polarity reversal, while the high-frequency component (**Ac**) does, as expected from the data and modelling. This can be understood by decomposing the signal into two components. The first component is governed by the bifurcation and termination density, and is filtered by the regular weighting function (**Ba**), which acts as a low-pass filter (**Bb**). The second component is governed by the fiber density, and is filtered by the derivative of the weighting function (**Bc**), which acts as a high- or band-pass filter (**Bd**).

Bibliophraphy

Buzsáki, György, Costas A. Anastassiou, and Christof Koch. 2012. "The origin of extracellular fields and currents — EEG, ECoG, LFP and spikes." *Nature Reviews Neuroscience* 13 (6). Nature Publishing Group: 407–20. doi:10.1038/nrn3241.

Gold, Carl, Darrell A. Henze, Christof Koch, and György Buzsáki. 2006. "On the origin of the extracellular action potential waveform: A modeling study." *Journal of Neurophysiology* 95 (5). Beckman Institute, 216-76, California Institute of Technology, Pasadena, CA 91125. carlg@caltech.edu).: 3113–28. doi:10.1152/jn.00979.2005.

Gydikov, A. A., and N. A. Trayanova. 1986. "Extracellular potentials of single active muscle fibres: Effects of finite fibre length." *Biological Cybernetics* 53 (6). Springer-Verlag: 363–72. doi:10.1007/bf00318202.

Gydikov, A., L. Gerilovsky, N. Radicheva, and N. Trayanova. 1986. "Influence of the muscle fibre end geometry on the extracellular potentials." *Biological Cybernetics* 54 (1). Springer-Verlag: 1–8. doi:10.1007/bf00337110.

Holt, Gary R., and Christof Koch. 1999. "Electrical Interactions via the Extracellular Potential Near Cell Bodies." *Journal of Computational Neuroscience* 6 (2). Kluwer Academic Publishers: 169–84. doi:10.1023/a:1008832702585.

Kuokkanen, Paula T., Hermann Wagner, Go Ashida, Catherine E. Carr, and Richard Kempter. 2010. "On the origin of the extracellular field potential in the nucleus laminaris of the barn owl (Tyto alba)." *Journal of Neurophysiology* 104 (4). American Physiological Society: 2274–90. doi:10.1152/jn.00395.2010.

Plonsey, R. 1977. "Action potential sources and their volume conductor fields." *Proceedings of the IEEE* 65 (5). Case Western Reserve University, Cleveland, OH; IEEE: 601–11. doi:10.1109/proc.1977.10539.

Reimann, Michael W., Costas A. Anastassiou, Rodrigo Perin, Sean L. Hill, Henry Markram, and Christof Koch. 2013. "A Biophysically Detailed Model of Neocortical Local Field Potentials Predicts the Critical Role of Active Membrane Currents." *Neuron* 79 (2). Cell Press, 375–90. doi:10.1016/j.neuron.2013.05.023.